

1 **1. TITLE PAGE**

2 **Seasonal variability in methane and nitrous oxide fluxes from tropical peatlands in the**  
3 **Western Amazon basin**

4

5 Teh, Yit Arn<sup>1\*</sup>, Murphy, Wayne A.<sup>2</sup>, Berrio, Juan-Carlos<sup>2</sup>, Boom, Arnould<sup>2</sup>, and Page, Susan E.<sup>2</sup>

6 <sup>1</sup> Institute of Biological and Environmental Sciences, University of Aberdeen

7 <sup>2</sup> Department of Geography, University of Leicester

8 \* Author to whom all correspondence should be addressed; email: [yateh@abdn.ac.uk](mailto:yateh@abdn.ac.uk)

## 9 2. ABSTRACT

10 The Amazon plays a critical role in global atmospheric budgets of methane (CH<sub>4</sub>) and nitrous  
11 oxide (N<sub>2</sub>O). However, while we have a relatively good understanding of the continental-scale  
12 flux of these greenhouse gases (GHGs), one of the key gaps in knowledge is the specific  
13 contribution of peatland ecosystems to the regional budgets of these GHGs. Here we report  
14 CH<sub>4</sub> and N<sub>2</sub>O fluxes from lowland tropical peatlands in the Pastaza-Marañón foreland basin  
15 (PMFB) in Peru, one of the largest peatland complexes in the Amazon basin. The goal of this  
16 research was to: quantify the range and magnitude of CH<sub>4</sub> and N<sub>2</sub>O fluxes from this region;  
17 assess seasonal trends in trace gas exchange; and determine the role of different  
18 environmental variables in driving GHG flux. Trace gas fluxes were determined from the most  
19 numerically-dominant peatland vegetation types in the region: forested vegetation, forested  
20 (short pole) vegetation, *Mauritia flexuosa*-dominated palm swamp, and mixed palm swamp.  
21 Data were collected in both wet and dry seasons over the course of four field campaigns from  
22 2012 to 2014. Diffusive CH<sub>4</sub> emissions averaged  $36.05 \pm 3.09$  mg CH<sub>4</sub>-C m<sup>-2</sup> d<sup>-1</sup> across the  
23 entire dataset, with diffusive CH<sub>4</sub> flux varying significantly among vegetation types and  
24 between seasons. The ebullition flux of CH<sub>4</sub> averaged  $973.3 \pm 161.4$  mg CH<sub>4</sub>-C m<sup>-2</sup> d<sup>-1</sup>, and did  
25 not vary significantly among vegetation types nor between seasons. Diffusive CH<sub>4</sub> flux was  
26 greatest for mixed palm swamp ( $52.0 \pm 16.0$  mg CH<sub>4</sub>-C m<sup>-2</sup> d<sup>-1</sup>), followed by *M. flexuosa* palm  
27 swamp ( $36.7 \pm 3.9$  mg CH<sub>4</sub>-C m<sup>-2</sup> d<sup>-1</sup>), forested (short pole) vegetation ( $31.6 \pm 6.6$  mg CH<sub>4</sub>-C m<sup>-2</sup>  
28 d<sup>-1</sup>), and forested vegetation ( $29.8 \pm 10.0$  mg CH<sub>4</sub>-C m<sup>-2</sup> d<sup>-1</sup>). Diffusive CH<sub>4</sub> flux also showed  
29 marked seasonality, with divergent seasonal patterns among ecosystems. Forested  
30 vegetation and mixed palm swamp showed significantly higher dry season ( $47.2 \pm 5.4$  mg CH<sub>4</sub>-  
31 C m<sup>-2</sup> d<sup>-1</sup> and  $85.5 \pm 26.4$  mg CH<sub>4</sub>-C m<sup>-2</sup> d<sup>-1</sup>, respectively) compared to wet season emissions

32 (6.8 ± 1.0 mg CH<sub>4</sub>-C m<sup>-2</sup> d<sup>-1</sup> and 5.2 ± 2.7 mg CH<sub>4</sub>-C m<sup>-2</sup> d<sup>-1</sup>, respectively). In contrast, forested  
33 (short pole) vegetation and *M. flexuosa* palm swamp showed the opposite trend, with dry  
34 season flux of 9.6 ± 2.6 and 25.5 ± 2.9 mg CH<sub>4</sub>-C m<sup>-2</sup> d<sup>-1</sup>, respectively, versus wet season flux  
35 of 103.4 ± 13.6 and 53.4 ± 9.8 mg CH<sub>4</sub>-C m<sup>-2</sup> d<sup>-1</sup>, respectively. These divergent seasonal trends  
36 may be linked to very high water tables (>1 m) in forested vegetation and mixed palm swamp  
37 during the wet season, which may have constrained CH<sub>4</sub> transport across the soil-atmosphere  
38 interface. Diffusive N<sub>2</sub>O flux was very low (0.70 ± 0.34 μg N<sub>2</sub>O-N m<sup>-2</sup> d<sup>-1</sup>), and did not vary  
39 significantly among ecosystems nor between seasons. We conclude that peatlands in the  
40 PMFB are large and regionally significant sources of atmospheric CH<sub>4</sub>, that need to be better  
41 accounted for in regional emissions inventories. In contrast, N<sub>2</sub>O flux was negligible,  
42 suggesting that this region does not make a significant contribution to regional atmospheric  
43 budgets of N<sub>2</sub>O. The divergent seasonal pattern in CH<sub>4</sub> flux among vegetation types challenges  
44 our underlying assumptions of the controls on CH<sub>4</sub> flux in tropical peatlands, and emphasizes  
45 the need for more process-based measurements during high water table periods.

46

47

#### 48 **KEYWORDS**

49 methane, nitrous oxide, peat, tropical peatland, Amazonia, Peru

50

51

52

### 53 3. INTRODUCTION

54 The Amazon basin plays a critical role in the global atmospheric budgets of carbon (C) and  
55 greenhouse gases (GHGs) such as methane (CH<sub>4</sub>) and nitrous oxide (N<sub>2</sub>O). Recent basin-wide  
56 studies suggest that the Amazon as a whole accounts for approximately 7 % of global  
57 atmospheric CH<sub>4</sub> emissions (Wilson et al., 2016). N<sub>2</sub>O emissions are of a similar magnitude,  
58 with emissions ranging from 2-3 Tg N<sub>2</sub>O-N year<sup>-1</sup> (or, approximately 12-18 % of global  
59 atmospheric emissions) (Huang et al., 2008;Saikawa et al., 2014;Saikawa et al., 2013). While  
60 we have a relatively strong understanding of the role that the Amazon plays in regional and  
61 global atmospheric budgets of these gases, one of the key gaps in knowledge is the  
62 contribution of specific ecosystem types to regional fluxes of GHGs (Huang et al.,  
63 2008;Saikawa et al., 2014;Saikawa et al., 2013). In particular, our understanding of the  
64 contribution of Amazonian wetlands to regional C and GHG budgets is weak, as the majority  
65 of past ecosystem-scale studies have focused on *terra firme* forests and savannas (D'Amelio  
66 et al., 2009;Saikawa et al., 2013;Wilson et al., 2016;Kirschke et al., 2013;Nisbet et al., 2014).  
67 Empirical studies of GHG fluxes from Amazonian wetlands are more limited in geographic  
68 scope and have focused on three major areas: wetlands in the state of Amazonas near the  
69 city of Manaus (Devol et al., 1990;Bartlett et al., 1990;Bartlett et al., 1988;Keller et al., 1986),  
70 the Pantanal region (Melack et al., 2004;Marani and Alvalá, 2007;Lienggaard et al., 2013), and  
71 the Orinoco River basin (Smith et al., 2000;Lavelle et al., 2014). Critically, none of the  
72 ecosystems sampled in the past were peat-forming ones; rather, the habitats investigated  
73 were non-peat forming (i.e. mineral or organo-mineral soils), seasonally-inundated floodplain  
74 forests (i.e. *varzea*), rivers or lakes.

75

76 Peatlands are one of the major wetland habitats absent from current bottom-up GHG  
77 inventories for the Amazon basin, and are often grouped together with non-peat forming  
78 wetlands in regional atmospheric budgets (Wilson et al., 2016). Unlike their Southeast Asian  
79 counterparts, most peatlands in the Amazon basin are unaffected by human activity at the  
80 current time (Lahteenoja et al., 2009a; Lahteenoja et al. 2009b; Lahteenoja and Page 2011),  
81 except for ecosystems in the Madre de Dios region in southeastern Peru, which are impacted  
82 by gold mining (Householder et al., 2012). Because we have little or no data on ecosystem-  
83 level land-atmosphere fluxes from Amazonian peatlands (Lahteenoja et al., 2012; Lahteenoja  
84 et al., 2009b; Kirschke et al., 2013; Nisbet et al., 2014), it is difficult to ascertain if rates of GHG  
85 flux from these ecosystems are similar to or different from mineral soil wetlands (e.g. *varzea*).  
86 Given that underlying differences in plant community composition and soil properties are  
87 known to modulate the cycling and flux of GHGs in wetlands (Limpens et al., 2008; Melton et  
88 al., 2013; Belyea and Baird, 2006; Sjögersten et al., 2014), expanding our observations to  
89 include a wider range of wetland habitats is critical in order to improve our understanding of  
90 regional trace gas exchange, and also to determine if aggregating peat and mineral soil  
91 wetlands together in bottom-up emissions inventories are appropriate for regional budget  
92 calculations. Moreover, Amazonian peatlands are thought to account for a substantial land  
93 area (i.e. up to 150,000 km<sup>2</sup>) (Schulman et al., 1999; Lahteenoja et al., 2012), and any  
94 differences in biogeochemistry among peat and mineral/organo-mineral soil wetlands may  
95 therefore have important implications for understanding and modelling the biogeochemical  
96 functioning of the Amazon basin as a whole.

97

98 Since the identification of extensive peat forming wetlands in the north (Lahteenoja et al.,  
99 2009a; Lahteenoja et al. 2009b; Lahteenoja and Page 2011) and south (Householder et al.,  
100 2012) of the Peruvian Amazon, several studies have been undertaken to better characterize  
101 these habitats, investigating vegetation composition and habitat diversity (Draper et al., 2014;  
102 Kelly et al., 2014; Householder et al., 2012; Lahteenoja and Page, 2011), vegetation history  
103 (Lahteenoja and Roucoux et al., 2010), C stocks (Lahteenoja et al., 2012; Draper et al., 2014),  
104 hydrology (Kelly et al., 2014), and peat chemistry (Lahteenoja et al., 2009a; Lahteenoja et al.,  
105 2009b). Most of the studies have focused on the Pastaza-Marañón foreland basin (PMFB),  
106 where one of the largest stretches of contiguous peatlands have been found (Lahteenoja et  
107 al 2009a; Lahteenoja and Page, 2011; Kelly et al, 2014), covering an estimated area of 35,600  
108  $\pm 2,133 \text{ km}^2$  (Draper et al., 2014). Up to 90% of the peatlands in the PMFB lie in flooded  
109 backwater river margins on floodplains and are influenced by large, annual fluctuations in  
110 water table caused by the Amazonian flood pulse (Householder et al., 2012; Lahteenoja et al.,  
111 2009a). These floodplain systems are dominated by peat deposits that range in depth from  
112  $\sim 3.9 \text{ m}$  (Lahteenoja et al., 2009a) to  $\sim 12.9 \text{ m}$  (Householder et al., 2012). The remaining 10%  
113 of these peatlands are not directly influenced by river flow and form domed (i.e. raised)  
114 nutrient-poor bogs that likely only receive water and nutrients from rainfall (Lahteenoja et  
115 al., 2009b). These nutrient-poor bogs are dominated by large, C-rich forests (termed “pole  
116 forests”), that represent a very high density C store (total pool size of  $1391 \pm 710 \text{ Mg C ha}^{-1}$ ,  
117 which includes both above- and belowground stocks); exceeding in fact the C density of  
118 nearby floodplain systems (Draper et al., 2014). Even though the peats in these nutrient-poor  
119 bogs have a relatively high hydraulic conductivity, they act as natural stores of water because  
120 of high rainwater inputs ( $>3000 \text{ mm}$  per annum), which help to maintain high water tables,  
121 even during parts of the dry season (Kelly et al., 2014).

122

123 CH<sub>4</sub> flux in tropical soils are regulated by the complex interplay among multiple factors that  
124 regulate CH<sub>4</sub> production, oxidation, and transport. Key factors include: redox/water table  
125 depth (Couwenberg et al., 2010;Couwenberg et al., 2011;Silver et al., 1999;Teh et al.,  
126 2005;von Fischer and Hedin, 2007), plant productivity (von Fischer and Hedin, 2007;Whiting  
127 and Chanton, 1993), soil organic matter lability (Wright et al., 2011), competition for C  
128 substrates among anaerobes (Teh et al., 2008;Teh and Silver, 2006;von Fischer and Hedin,  
129 2007), and presence of plants capable of facilitating atmospheric egress (Pangala et al., 2013).  
130 Of all these factors, fluctuation in soil redox conditions, as mediated by variations in water  
131 table depth, is perhaps most critical in regulating CH<sub>4</sub> dynamics (Couwenberg et al.,  
132 2010;Couwenberg et al., 2011), because of the underlying physiology of the microbes that  
133 produce and consume CH<sub>4</sub>. Methanogenic archaea are obligate anaerobes that only produce  
134 CH<sub>4</sub> under anoxic conditions (Conrad, 1996); as a consequence, they are only active in stably  
135 anoxic soil microsites or soil layers, where they are protected from the effects of strong  
136 oxidants such as oxygen or where competition for reducing equivalents (e.g. acetate, H<sub>2</sub>) from  
137 other anaerobic microorganisms is eliminated (Teh et al., 2008;Teh and Silver, 2006;Teh et  
138 al., 2005;von Fischer and Hedin, 2002;von Fischer and Hedin, 2007). CH<sub>4</sub> oxidation, on the  
139 other hand, is thought to be driven primarily by aerobic methanotrophic bacteria in tropical  
140 soils (Hanson and Hanson, 1996;Teh et al., 2005;Teh et al., 2006;von Fischer and Hedin,  
141 2002;von Fischer and Hedin, 2007), with anaerobic CH<sub>4</sub> oxidation playing a quantitatively  
142 smaller role (Blazewicz et al., 2012). Thus, fluctuations in redox or water table depth play a  
143 fundamental role in directing the flow of C among different anaerobic pathways (Teh et al.,  
144 2008;Teh and Silver, 2006;von Fischer and Hedin, 2007), and shifting the balance between

145 production and consumption of CH<sub>4</sub> (Teh et al., 2005; von Fischer and Hedin, 2002). Moreover,  
146 water table or soil moisture fluctuations are also thought to profoundly influence CH<sub>4</sub>  
147 transport dynamics throughout the soil profile, changing the relative partitioning of CH<sub>4</sub>  
148 among different transport pathways such as diffusion, ebullition, and plant-facilitated  
149 transport (Whalen, 2005; Jungkunst and Fiedler, 2007).

150

151 Controls on N<sub>2</sub>O flux are also highly complex (Groffman et al., 2009), with N<sub>2</sub>O originating  
152 from as many as four separate sources (e.g. bacterial ammonia oxidation, archaeal ammonia  
153 oxidation, denitrification, dissimilatory nitrate reduction to ammonium), each with different  
154 environmental controls (Baggs, 2008; Morley and Baggs, 2010; Firestone and Davidson,  
155 1989; Firestone et al., 1980; Pett-Ridge et al., 2013; Silver et al., 2001; Prosser and Nicol, 2008).  
156 Key factors regulating soil N<sub>2</sub>O flux include: redox, soil moisture content or water table depth,  
157 temperature, pH, labile C availability, and labile N availability (Groffman et al., 2009). As is the  
158 case for CH<sub>4</sub>, variations in redox/water table depth plays an especially prominent role in  
159 regulating N<sub>2</sub>O flux in tropical peatland ecosystems, because all of the processes that produce  
160 N<sub>2</sub>O are redox-sensitive, with bacterial or archaeal ammonia oxidation occurring under  
161 aerobic conditions (Prosser and Nicol, 2008; Firestone and Davidson, 1989; Firestone et al.,  
162 1980) whereas nitrate-reducing processes (i.e. denitrification, dissimilatory nitrate reduction  
163 to ammonium) are anaerobic ones (Firestone and Davidson, 1989; Firestone et al.,  
164 1980; Morley and Baggs, 2010; Silver et al., 2001). Moreover, for nitrate reducing processes,  
165 which are believed to be the dominant source of N<sub>2</sub>O in wet systems, the extent of  
166 anaerobiosis also controls the relative proportion of N<sub>2</sub>O or N<sub>2</sub> produced during dissimilatory



167 metabolism (Firestone and Davidson, 1989; Firestone et al., 1980; Morley and Baggs,  
168 2010; Silver et al., 2001).

169

170 In order to improve our understanding of the biogeochemistry and rates of GHG exchange  
171 from Amazonian peatlands, we conducted a preliminary study of CH<sub>4</sub> and N<sub>2</sub>O fluxes from  
172 forested peatlands in the PMFB. The main objectives of this are to:

- 173 1. Quantify the magnitude and range of soil CH<sub>4</sub> and N<sub>2</sub>O fluxes from a sub-set of  
174 peatlands in the PMFB that represent dominant vegetation types
- 175 2. Determine seasonal patterns of trace gas exchange
- 176 3. Establish the relationship between trace gas fluxes and environmental variables

177 Sampling was concentrated on the four most dominant vegetation types in the area, based  
178 on prior work by the investigators (Lahteenoja and Page, 2011). Trace gas fluxes were  
179 captured from both floodplain systems and nutrient-poor bogs in order to account for  
180 underlying differences in biogeochemistry that may arise from variations in hydrology.  
181 Sampling was conducted during four field campaigns (two wet season, two dry season) over  
182 a 27-month period, extending from February 2012 to May 2014.

183

184

## 185 **4. MATERIALS AND METHODS**

### 186 **4.1 Study site and sampling design**

187 The study was carried out in the lowland tropical peatland forests of the PMFB, between 2  
188 and 35 km south of the city of Iquitos, Peru (Lahteenoja et al., 2009a; Lahteenoja et al., 2009b)  
189 (Figure 1, Table 1). The mean annual temperature is 26 °C, annual precipitation is c. 3,100  
190 mm, relative humidity ranges from 80-90 %, and altitude ranges from c. 90 to 130 m above  
191 sea level (Marengo 1998). The northwestern Amazon basin near Iquitos experiences  
192 pronounced seasonality, which is characterized by consistently high annual temperatures, but  
193 marked seasonal variation in precipitation (Tian et al., 1998), and an annual river flood pulse  
194 linked to seasonal discharge from the Andes (Junk et al., 1989). Precipitation events are  
195 frequent, intense and of significant duration during the wet season (November to May) and  
196 infrequent, intense and of short duration during the dry season (June to August). September  
197 and October represent a transitional period between dry and wet seasons, where rainfall  
198 patterns are less predictable. Catchments in this region receive no less than 100 mm of rain  
199 per month (Espinoza Villar et al., 2009a; Espinoza Villar et al., 2009b) and >3000 mm of rain  
200 per year. River discharge varies by season, with the lowest discharge between the dry season  
201 months of August and September. Peak discharge from the wet season flood pulse occurs  
202 between April and May, as recorded at the Tamshiyaku River gauging station (Espinoza Villar  
203 et al., 2009b).

204

205 Histosols form the dominant soil type for peatlands in this region (Andriessse, 1988;Lahteenoja  
206 and Page, 2011). Study sites are broadly classified as nutrient-rich, intermediate, or nutrient-  
207 poor (Lahteenoja and Page, 2011), with pH ranging from 3.5 to 7.2 (Lahteenoja and Page,  
208 2011;Lahteenoja et al., 2009a;Lahteenoja et al., 2009b). More specific data on pH for our plots  
209 are presented in Table 3. Nutrient-rich (i.e. minerotrophic) sites tend to occur on floodplains

210 and river margins, and account for at least 60 % of the peatland cover in the PMFB (Lahteenoja  
211 and Page, 2011;Draper et al., 2014). They receive water, sediment, and nutrient inputs from  
212 the annual Amazon river flood pulse (Householder et al., 2012;Lahteenoja and Page, 2011),  
213 leading to higher inorganic nutrient content, of which Ca and other base cations form major  
214 constituents (Lahteenoja and Page, 2011). Many of the soils in these nutrient-rich areas are  
215 fluvaquentic Tropofibrists (Andriessse, 1988), and contain thick mineral layers or minerogenic  
216 intrusions, reflective of episodic sedimentation events in the past (Lahteenoja and Page,  
217 2011). In contrast, nutrient-poor (i.e. oligotrophic) sites tend to occur further in-land  
218 (Lahteenoja and Page, 2011;Draper et al., 2014). They are almost entirely rain-fed, and  
219 receive low or infrequent inputs of water and nutrients from streams and rivers (Lahteenoja  
220 and Page, 2011). These ecosystems account for 10 to 40 % of peatland cover in the PMFB,  
221 though precise estimates vary depending on the land classification scheme employed  
222 (Lahteenoja and Page, 2011;Draper et al., 2014). Soil Ca and base cation concentrations are  
223 significantly lower in these sites compared to nutrient-rich ones, with similar concentrations  
224 to that of rainwater (Lahteenoja and Page, 2011). Soils are classified as typic or hydric  
225 Tropofibrists (Andriessse, 1988). Even though Ca and base cations themselves play no direct  
226 role in modulating CH<sub>4</sub> and N<sub>2</sub>O fluxes, underlying differences in soil fertility may indirectly  
227 influence CH<sub>4</sub> and N<sub>2</sub>O flux by influencing the rate of labile C input to the soil, the  
228 decomposability of organic matter, and the overall throughput of C and nutrients through the  
229 plant-soil system (Firestone and Davidson, 1989;Groffman et al., 2009;von Fischer and Hedin,  
230 2007;Whiting and Chanton, 1993).

231

232 We established 239 sampling plots ( $\sim 30 \text{ m}^2$  per plot) within five tropical peatland sites that  
233 captured four of the dominant vegetation types in the region (Draper et al.,  
234 2014;Householder et al., 2012;Kelly et al., 2014;Lahteenoja and Page, 2011), and which  
235 encompassed a range of nutrient availabilities (Figure 1, Table 1) (Lahteenoja and Page,  
236 2011;Lahteenoja et al., 2009a). These four dominant vegetation types included: forested  
237 vegetation (nutrient-rich; n= 21 plots), forested (short pole) vegetation (nutrient-poor; n= 47  
238 plots), *Mauritia flexuosa*-dominated palm swamp (intermediate fertility, n= 153 plots), and  
239 mixed palm swamp (nutrient-rich; n=18 plots) (Table 1). Four of the study sites (Buena Vista,  
240 Charo, Miraflores, and Quistococha) were dominated by only one vegetation type, whereas  
241 San Jorge contained a mixture of *M. flexuosa* palm swamp and forested (short pole)  
242 vegetation (Table 1). As a consequence, both vegetation types were sampled in San Jorge to  
243 develop a more representative picture of GHG fluxes from this location. Sampling efforts were  
244 partially constrained by issues of site access; some locations were difficult to access (e.g.  
245 centre of the San Jorge peatland) due to water table height and navigability of river channels;  
246 as a consequence, sampling patterns were somewhat uneven, with higher sampling densities  
247 in some peatlands than in others (Table 1).

248

249 In each peatland site, transects were established from the edge of the peatland to its centre.  
250 Each transect varied in length from 2 to 5 km, depending on the relative size of the peatland.  
251 Randomly located sampling plots ( $\sim 30 \text{ m}^2$  per plot) were established at 50 or 200 m intervals  
252 along each transect, from which GHG fluxes and environmental variables were measured  
253 concomitantly. The sampling interval (i.e. 50 or 200 m) was determined by the length of the  
254 transect or size of the peatland, with shorter sampling intervals (50 m) for shorter transects

255 (i.e. smaller peatlands) and longer sampling intervals (200 m) for longer transects (i.e. larger  
256 peatlands).

257

## 258 **4.2 Quantifying soil-atmosphere exchange**

259 Soil-atmosphere fluxes (CH<sub>4</sub>, N<sub>2</sub>O) were determined in four campaigns over a two-year annual  
260 water cycle: February 2012 (wet season), June-August 2012 (dry season), June-July 2013 (dry  
261 season), and May-June 2014 (wet season). The duration of the campaign for each study site  
262 varied depending on its size. Each study site was generally sampled only once for each  
263 campaign, except for a sub-set of plots within each vegetation type where diurnal studies  
264 were conducted to determine if CH<sub>4</sub> and N<sub>2</sub>O fluxes varied over daily time steps. Gas exchange  
265 was quantified using a floating static chamber approach (Livingston and Hutchinson, 1995;  
266 Teh et al., 2011). Static flux measurements were made by enclosing a 0.225 m<sup>2</sup> area with a  
267 dark, single component, vented 10 L flux chamber. No chamber bases (collars) were used due  
268 to the highly saturated nature of the soils. In most cases, a standing water table was present  
269 at the soil surface, so chambers were placed directly onto the water. In the absence of a  
270 standing water table, a weighted skirt was applied to create an airtight seal. Under these drier  
271 conditions, chambers were placed carefully on the soil surface. In order to reduce the risk of  
272 pressure-induced ebullition or disruption to soil gas concentration profiles caused by the  
273 investigators' footfall, flux chambers were lowered from a distance of 2-m away using a 2-m  
274 long pole. Gas samples were collected with syringes using >2 m lengths of Tygon® tubing,  
275 after thoroughly purging the dead volumes in the sample lines. To promote even mixing  
276 within the headspace, chambers were fitted with small computer fans (Pumpanen et al.,  
277 2004). Headspace samples were collected from each flux chamber at five intervals over a 25

278 minute enclosure period using a gas tight syringe. Gas samples were stored in evacuated  
279 Exetainers® (Labco Ltd., Lampeter UK), shipped to the UK, and subsequently analysed for CH<sub>4</sub>,  
280 CO<sub>2</sub> and N<sub>2</sub>O concentrations using Thermo TRACE GC Ultra (Thermo Fischer Scientific Inc.,  
281 Waltham, Massachusetts, USA) at the University of St. Andrews. Chromatographic separation  
282 was achieved using a Porapak-Q column, and gas concentrations determined using a flame  
283 ionization detector (FID) for CH<sub>4</sub>, a methanizer-FID for CO<sub>2</sub>, and an electron capture detector  
284 (ECD) for N<sub>2</sub>O. Instrumental precision, determined from repeated analysis of standards, was  
285 < 5% for all detectors.

286

287 Diffusive fluxes were determined by using the JMP IN version 11 (SAS Institute, Inc., Cary,  
288 North Carolina, USA) statistical package to plot best-fit lines to the data for headspace  
289 concentration against time for individual flux chambers, with fluxes calculated from linear or  
290 non-linear regressions depending on the individual concentration trend against time (Teh et  
291 al., 2014). Gas mixing ratios (ppm) were converted to areal fluxes by using the Ideal Gas Law  
292 to solve for the quantity of gas in the headspace (on a mole or mass basis) and normalized by  
293 the surface area of each static flux chamber (Livingston and Hutchinson, 1995). Ebullition-  
294 derived CH<sub>4</sub> fluxes were also quantified in our chambers where evidence of ebullition was  
295 found. This evidence consisted of either: (i) rapid, non-linear increases in CH<sub>4</sub> concentration  
296 over time; (ii) abrupt, stochastic increases in CH<sub>4</sub> concentration over time; or (iii) an abrupt  
297 stochastic increase in CH<sub>4</sub> concentration, followed by a linear decline in concentration. For  
298 observations following pattern (i), flux was calculated by fitting a quadratic regression  
299 equation to the data ( $P < 0.05$ ), and CH<sub>4</sub> flux determined from the initial steep rise in CH<sub>4</sub>  
300 concentration. For data following pattern (ii), the ebullition rate was determined by

301 calculating the total CH<sub>4</sub> production over the course of the bubble event, in-line with prior  
302 work conducted by the investigators (Teh et al., 2011). Last, for data following pattern (iii), a  
303 best-fit line was plotted to the CH<sub>4</sub> concentration data after the bubble event, and a net rate  
304 of CH<sub>4</sub> uptake calculated from the gradient of the line. Observations following patterns (i) and  
305 (ii) were categorized as “ebullition” (i.e. net efflux) whereas observations following pattern  
306 (iii) were categorized as “ebullition-driven CH<sub>4</sub> uptake” (i.e. net influx).

307

### 308 **4.3 Environmental variables**

309 To investigate the effects of environmental variables on trace gas fluxes, we determined air  
310 temperature, soil temperature, chamber headspace temperature, soil pH, soil electrical  
311 conductivity (EC;  $\mu\text{Scm}^{-2}$ ), dissolved oxygen concentration of the soil pore water (DO;  
312 measured as percent saturation, %) in the top 15 cm of the peat column, and water table  
313 position concomitant with gas sampling. Air temperature (measured 1.3 m above the soil)  
314 and chamber headspace temperature were measured using a Checktemp<sup>®</sup> probe and meter  
315 (Hanna Instruments LTD, Leighton Buzzard, UK). Peat temperature, pH, DO and EC were  
316 measured at a depth of 15 cm below the peat surface and recorded *in situ* with each gas  
317 sample using a HACH<sup>®</sup> rugged outdoor HQ30D multi meter and pH, LDO or EC probe. At sites  
318 where the water level was above the peat surface, the water depth was measured using a  
319 meter rule. Where the water table was at or below the peat surface, the water level was  
320 measured by auguring a hole to 1 m depth and measuring water table depth using a meter  
321 rule.

322

## 323 **4.4 Statistical Analyses**

324 Statistical analyses were performed using JMP IN version 11 (SAS Institute, Inc., Cary, North  
325 Carolina, USA). Box-Cox transformations were applied where the data failed to meet the  
326 assumptions of analysis of variance (ANOVA); otherwise, non-parametric tests were applied  
327 (e.g. Wilcoxon signed-rank test). ANOVA and analysis of co-variance (ANCOVA) were used to  
328 test for relationships between gas fluxes and vegetation type, season, and environmental  
329 variables. When determining the effect of vegetation type on gas flux, data from different  
330 study sites (e.g. San Jorge and Miraflores) were pooled together. Means comparisons were  
331 tested using a Fisher's Least Significant Difference (LSD) test.

332

333

## 334 **5. RESULTS**

### 335 **5.1 Differences in gas fluxes and environmental variables among vegetation types**

336 All vegetation types were net sources of CH<sub>4</sub>, with an overall mean ( $\pm$  standard error) diffusive  
337 flux of  $36.1 \pm 3.1$  mg CH<sub>4</sub>-C m<sup>-2</sup> d<sup>-1</sup> and a mean ebullition flux of  $973.3 \pm 161.4$  mg CH<sub>4</sub>-C m<sup>-2</sup>  
338 d<sup>-1</sup> (Figure 2, Table 2). We also saw examples of ebullition-driven CH<sub>4</sub> uptake (i.e. a sudden or  
339 stochastic increase in CH<sub>4</sub> concentration, followed immediately by a rapid linear decline in  
340 concentration), with a mean rate of  $-504.1 \pm 84.4$  mg CH<sub>4</sub>-C m<sup>-2</sup> d<sup>-1</sup> (Table 2). Diffusive fluxes  
341 of CH<sub>4</sub> accounted for the majority of observations (83.3 to 93.1 %), while ebullition or  
342 ebullition-driven uptake of CH<sub>4</sub> accounted for a much smaller proportion of observations (6.9  
343 to 16.7 %; Table 2).



344

345 Diffusive CH<sub>4</sub> flux varied significantly among the four vegetation types sampled in this study  
346 (two-way ANOVA with vegetation, season and their interaction,  $F_{7, 979} = 13.2$ ,  $P < 0.0001$ ; Fig.  
347 2a). However, the effect of vegetation was relatively weak (see ANCOVA results in the section  
348 'Relationships between gas fluxes and environmental variables'), and a means comparison  
349 test on the pooled data was unable to determine which means differed significantly from the  
350 others (Fisher's LSD,  $P > 0.05$ ). For the pooled data, the overall numerical trend was that mixed  
351 palm swamp showed the highest mean flux ( $52.0 \pm 16.0$  mg CH<sub>4</sub>-C m<sup>-2</sup> d<sup>-1</sup>), followed by *M.*  
352 *flexuosa* palm swamp ( $36.7 \pm 3.9$  mg CH<sub>4</sub>-Cm<sup>-2</sup> d<sup>-1</sup>), forested (short pole) vegetation ( $31.6 \pm$   
353  $6.6$  mg CH<sub>4</sub>-Cm<sup>-2</sup> d<sup>-1</sup>), and forested vegetation ( $29.8 \pm 10.0$  mg CH<sub>4</sub>-C m<sup>-2</sup> d<sup>-1</sup>). CH<sub>4</sub> ebullition  
354 and ebullition-driven CH<sub>4</sub> uptake did not vary significant among vegetation types nor between  
355 seasons (Table 2).

356

357 These study sites were also a weak net source of N<sub>2</sub>O, with a mean diffusive flux of  $0.70 \pm 0.34$   
358  $\mu\text{g N}_2\text{O-N m}^{-2} \text{d}^{-1}$ . We saw only limited evidence of ebullition of N<sub>2</sub>O, with only three chambers  
359 out of 1181 (0.3 % of observations) showing evidence of N<sub>2</sub>O ebullition. These data were  
360 omitted from the analysis of diffusive flux of N<sub>2</sub>O. Because of the high variance in diffusive  
361 N<sub>2</sub>O flux among plots, analysis of variance indicated that mean diffusive N<sub>2</sub>O flux did not differ  
362 significantly among vegetation types (two-way ANOVA,  $P > 0.5$ , Fig. 2b). However, when the  
363 N<sub>2</sub>O flux data were grouped by vegetation type, we see that some vegetation types tended  
364 to function as net atmospheric sources, while others acted as atmospheric sinks (Fig. 2b, Table  
365 3). For example, the highest N<sub>2</sub>O emissions were observed from *M. flexuosa* palm swamp  
366 ( $1.11 \pm 0.44$   $\mu\text{g N}_2\text{O-N m}^{-2} \text{d}^{-1}$ ) and forested vegetation ( $0.20 \pm 0.95$   $\mu\text{g N}_2\text{O-N m}^{-2} \text{d}^{-1}$ ). In

367 contrast, forested (short pole) vegetation and mixed palm swamp were weak sinks for N<sub>2</sub>O,  
368 with a mean flux of  $-0.01 \pm 0.84$  and  $-0.21 \pm 0.70 \mu\text{g N}_2\text{O-N m}^{-2} \text{d}^{-1}$ , respectively.

369

370 Soil pH varied significantly among vegetation types (data pooled across all seasons; ANOVA,  
371  $P < 0.0001$ , Table 3). Multiple comparisons tests indicated that mean soil pH was significantly  
372 different for each of the vegetation types (Fisher's LSD,  $P < 0.0001$ , Table 3), with the lowest  
373 pH in forested (short pole) vegetation ( $4.10 \pm 0.04$ ), followed by *M. flexuosa* palm swamp  
374 ( $5.32 \pm 0.02$ ), forested vegetation ( $6.15 \pm 0.06$ ), and the mixed palm swamp ( $6.58 \pm 0.04$ ).

375

376 Soil dissolved oxygen (DO) content varied significantly among vegetation types (data pooled  
377 across all seasons; Kruskal-Wallis,  $P < 0.0001$ , Table 3). Multiple comparisons tests indicated  
378 that mean DO was significantly different for each of the vegetation types (Fisher's LSD,  $P <$   
379  $0.05$ , Table 3), with the highest DO in the forested (short pole) vegetation ( $25.2 \pm 2.1 \%$ ),  
380 followed by the *M. flexuosa* palm swamp ( $18.1 \pm 1.0 \%$ ), forested vegetation ( $11.8 \pm 2.8 \%$ ),  
381 and the mixed palm swamp ( $0.0 \pm 0.0 \%$ ).

382

383 Electrical conductivity (EC) varied significantly among vegetation types (data pooled across all  
384 seasons; Kruskal-Wallis,  $P < 0.0001$ , Table 3). Multiple comparison tests indicated that mean  
385 EC was significantly different for each of the vegetation types (Fisher's LSD,  $P < 0.05$ ; Table 3),  
386 with the highest EC in the mixed palm swamp ( $170.9 \pm 6.0 \mu\text{s m}^{-2}$ ), followed by forested  
387 vegetation ( $77.1 \pm 4.2 \mu\text{s m}^{-2}$ ), *M. flexuosa* palm swamp ( $49.7 \pm 1.4 \mu\text{s m}^{-2}$ ) and the forested  
388 (short pole) vegetation ( $40.9 \pm 3.5 \mu\text{s m}^{-2}$ ).

389

390 Soil temperature varied significantly among vegetation types (data pooled across all seasons;  
391 ANOVA,  $P < 0.0001$ , Table 3). Multiple comparisons tests indicated that soil temperature in  
392 forested (short pole) vegetation was significantly lower than in the other vegetation types  
393 (Table 3); whereas the other vegetation types did not differ in temperature amongst  
394 themselves (Fisher's LSD,  $P < 0.05$ , Table 3).

395

396 Air temperature varied significantly among vegetation types (data pooled across all seasons;  
397 ANOVA,  $P < 0.0001$ , Table 3). Multiple comparisons tests indicated that air temperature in *M.*  
398 *flexuosa* palm swamp was significantly lower than in the other vegetation types; whereas the  
399 other vegetation types did not differ in temperature amongst themselves (Fisher's LSD,  $P <$   
400  $0.05$ , Table 3).

401

402 Water table depths varied significantly among vegetation types (data pooled across all  
403 seasons; ANOVA,  $P < 0.0001$ , Table 3). The highest mean water tables were observed in mixed  
404 palm swamp ( $59.6 \pm 9.3$  cm), followed by forested vegetation ( $34.0 \pm 6.9$  cm), *M. flexuosa*  
405 palm swamp ( $17.4 \pm 1.2$  cm), and forested (short pole) vegetation ( $3.5 \pm 1.0$  cm) (Fisher's LSD,  
406  $P < 0.0005$ ).

407

408 **5.2 Temporal variations in gas fluxes and environmental variables**

409 The peatlands sampled in this study showed pronounced seasonal variability in diffusive CH<sub>4</sub>  
410 flux (two-way ANOVA,  $F_{7, 979} = 13.2$ ,  $P < 0.0001$ ; Table 4). For ebullition of CH<sub>4</sub> and ebullition-  
411 driven uptake of CH<sub>4</sub>, mean fluxes varied between seasons, but high variability meant that  
412 these differences were not statistically significant ((two-way ANOVA,  $P > 0.8$ ; Table 2).  
413 Diffusive N<sub>2</sub>O flux showed no seasonal trends (two-way ANOVA,  $P > 0.5$ ), and therefore will  
414 not be discussed further here. Diurnal studies suggest that neither diffusive fluxes of CH<sub>4</sub> nor  
415 N<sub>2</sub>O varied over the course of a 24-hour period.

416

417 For diffusive CH<sub>4</sub> flux, the overall trend was towards significantly higher wet season ( $51.1 \pm$   
418  $7.0 \text{ mg CH}_4\text{-C m}^{-2} \text{ d}^{-1}$ ) compared to dry season ( $27.3 \pm 2.7 \text{ mg CH}_4\text{-C m}^{-2} \text{ d}^{-1}$ ) flux (data pooled  
419 across all vegetation types; t-Test,  $P < 0.001$ , Table 4). However, when diffusive CH<sub>4</sub> flux was  
420 disaggregated by vegetation type, very different seasonal trends emerged. For example, both  
421 forested vegetation and mixed palm swamp showed significantly greater diffusive CH<sub>4</sub> flux  
422 during the *dry season* with net fluxes of  $47.2 \pm 5.4 \text{ mg CH}_4\text{-C m}^{-2} \text{ d}^{-1}$  and  $64.2 \pm 12.1 \text{ mg CH}_4\text{-}$   
423  $\text{C m}^{-2} \text{ d}^{-1}$ , respectively (Fisher's LSD,  $P < 0.05$ , Table 3). In contrast, *wet season* flux was 7-16  
424 times lower, with net fluxes of  $6.7 \pm 1.0 \text{ mg CH}_4\text{-C m}^{-2} \text{ d}^{-1}$  and  $6.1 \pm 1.3 \text{ mg CH}_4\text{-C m}^{-2} \text{ d}^{-1}$ ,  
425 respectively (Fisher's LSD,  $P < 0.05$ , Table 3). In contrast, forested (short pole) vegetation and  
426 *M. flexuosa* palm swamp showed seasonal trends consistent with the pooled data set; i.e.  
427 significantly higher flux during the wet season ( $46.7 \pm 8.4$  and  $60.4 \pm 9.1 \text{ mg CH}_4\text{-C m}^{-2} \text{ d}^{-1}$ ,  
428 respectively) compared to the dry season ( $28.3 \pm 2.6$  and  $18.8 \pm 2.6 \text{ mg CH}_4\text{-C m}^{-2} \text{ d}^{-1}$ ,  
429 respectively) (Fisher's LSD,  $P < 0.05$ , Table 3).

430

431 Even though seasonal trends in CH<sub>4</sub> ebullition and ebullition-driven uptake were not  
432 statistically significant, we will briefly describe the overall patterns for the different  
433 vegetation types as they varied among ecosystems (Table 2). Forested vegetation showed no  
434 evidence of ebullition at all, while ebullition-driven uptake was greater during the dry season.  
435 For forested (short pole) vegetation, ebullition was generally greater during the wet season,  
436 while ebullition-driven uptake was higher during the dry season. For *M. flexuosa* palm swamp,  
437 both ebullition and ebullition-driven uptake were greater during the wet season. Lastly, for  
438 mixed palm swamp, both ebullition and ebullition-driven uptake were greater during the dry  
439 season.

440

441 For the environmental variables, soil pH, DO, EC, water table depth, and soil temperature  
442 varied significantly between seasons, whereas air temperature did not. Thus, for sake of  
443 brevity, air temperature is not discussed further here. Mean soil pH was significantly lower  
444 during the wet season ( $5.18 \pm 0.03$ ) than during the dry season ( $5.31 \pm 0.04$ ) (data pooled  
445 across all vegetation types; t-Test,  $P < 0.05$ , Table 2). When disaggregated by vegetation type,  
446 the overall trend was found to hold true for all vegetation types except forested (short pole)  
447 vegetation, which displayed higher pH during the wet season compared to the dry season  
448 (Table 2). A two-way ANOVA on Box-Cox transformed data using vegetation type, season and  
449 their interaction as explanatory variables indicated that vegetation type was the best  
450 predictor of pH, with season and vegetation type by season playing a lesser role ( $F_{7, 1166} =$   
451  $348.9$ ,  $P < 0.0001$ ).

452

453 For DO, the overall trend was towards significantly lower DO during the wet season ( $13.9 \pm$   
454  $1.0 \%$ ) compared to the dry season ( $19.3 \pm 1.2 \%$ ) (data pooled across all vegetation types;  
455 Wilcoxon test,  $P < 0.0001$ , Table 2). However, when the data were disaggregated by  
456 vegetation type, we found that individual vegetation types showed distinct seasonal trends  
457 from each other. Forested vegetation and mixed palm swamp were consistent with the  
458 overall trend (i.e. lower wet season compared to dry season DO), whereas forested (short  
459 pole) vegetation and *M. flexuosa* palm swamp displayed the reverse trend (i.e. higher *wet*  
460 *season* compared to *dry season* DO) (Table 2). A two-way ANOVA on Box Cox transformed  
461 data using vegetation type, season and their interaction as explanatory variables indicated  
462 that vegetation type was the best predictor of DO, followed by a strong vegetation by season  
463 interaction; season itself played a lesser role than either of the other two explanatory  
464 variables ( $F_{7, 1166} = 57.0$ ,  $P < 0.0001$ ).

465

466 For EC, the overall trend was towards lower EC in the wet season ( $49.4 \pm 1.8 \mu\text{s m}^{-2}$ ) compared  
467 to the dry season ( $65.5 \pm 2.2 \mu\text{s m}^{-2}$ ) (data pooled across all vegetation types; Wilcoxon test,  
468  $P < 0.05$ , Table 2). When the data were disaggregated by vegetation type, this trend was  
469 consistent for all the vegetation types except for forested vegetation, where differences  
470 between wet and dry season were not statistically significant (Wilcoxon,  $P > 0.05$ , Table 2).

471

472 Water table depths varied significantly between seasons (data pooled across all vegetation  
473 types; Wilcoxon test,  $P < 0.0001$ , Table 2). Mean water table level was significantly higher in  
474 the wet ( $54.1 \pm 2.7 \text{ cm}$ ) than the dry ( $1.3 \pm 0.8 \text{ cm}$ ) season. When disaggregated by vegetation

475 type, the trend held true for individual vegetation types (Table 2). All vegetation types had  
476 negative dry season water tables (i.e. below the soil surface) and positive wet season water  
477 tables (i.e. water table above the soil surface), except for *M. flexuosa* palm swamp that had  
478 positive water tables in both seasons. Two-way ANOVA on Box-Cox transformed data using  
479 vegetation type, season and their interaction as explanatory variables indicated that all three  
480 factors explained water table depth, but that season accounted for the largest proportion of  
481 the variance in the model, followed by vegetation by season, and lastly by vegetation type ( $F_{7,}$   
482  $_{1157} = 440.1, P < 0.0001$ ).

483

484 For soil temperature, the overall trend was towards slightly higher temperatures in the wet  
485 season ( $25.6 \pm 0.0$  °C) compared to the dry season ( $25.1 \pm 0.0$  °C) (t-Test,  $P < 0.0001$ ). Analysis  
486 of the disaggregated data indicates this trend was consistent for individual vegetation types  
487 (Table 2). Two-way ANOVA on Box-Cox transformed data using vegetation type, season and  
488 their interaction as explanatory variables indicated that all three variables played a significant  
489 role in modulating soil temperature, although season accounted for the largest proportion of  
490 the variance whereas the other two factors accounted for a similar proportion of the variance  
491 ( $F_{7, 1166} = 21.3, P < 0.0001$ ).

492

### 493 **5.3 Relationships between gas fluxes and environmental variables**

494 To explore the relationships between environmental variables and diffusive gas fluxes, we  
495 conducted an analysis of covariance (ANCOVA) on Box-Cox transformed gas flux data, using  
496 vegetation type, season, vegetation by season, and environmental variables as explanatory

497 variables. We did not analyze trends between ebullition and ebullition-driven uptake and  
498 environmental variables because of the limitations in the sampling methodology and the  
499 limited number of observations.

500

501 For diffusive CH<sub>4</sub> flux, ANCOVA revealed that vegetation by season was the strongest  
502 predictor of CH<sub>4</sub> flux, followed by a strong season effect ( $F_{13, 917} = 9.2, P < 0.0001$ ). Other  
503 significant drivers included soil temperature, water table depth, and a borderline-significant  
504 effect of vegetation type ( $P < 0.06$ ). However, it is important to note that each of these  
505 environmental variables were only weakly correlated with CH<sub>4</sub> flux even if the relationships  
506 were statistically significant; for example, when individual bivariate regressions were  
507 calculated, the  $r^2$  values were less than 0.01 for each plot (see Supplementary Online  
508 Materials, Figures S1 and S2).

509

510 For diffusive N<sub>2</sub>O flux, ANCOVA indicated that the best predictors of flux rates were dissolved  
511 oxygen and electrical conductivity ( $F_{13, 1014} = 2.2, P < 0.0082$ ). As was the case for CH<sub>4</sub>, when  
512 the relationships between these environmental variables and N<sub>2</sub>O flux were explored using  
513 individual bivariate regressions,  $r^2$  values were found to be very low (e.g. less than  $r^2 < 0.0007$ )  
514 or not statistically significant (see Supplementary Online Materials, Figures S3 and S4).

515

516

## 517 **6. DISCUSSION**



518 **6.1 Large and asynchronous CH<sub>4</sub> fluxes from peatlands in the Pastaza-Marañón foreland**  
519 **basin**

520 The ecosystems sampled in this study were strong atmospheric sources of CH<sub>4</sub>. Diffusive CH<sub>4</sub>  
521 flux, averaged across all vegetation types, was  $36.1 \pm 3.1$  mg CH<sub>4</sub>-C m<sup>-2</sup> d<sup>-1</sup>, spanning a range  
522 from -100 to 1,510 mg CH<sub>4</sub>-C m<sup>-2</sup> d<sup>-1</sup>. This mean falls within the range of other diffusive fluxes  
523 observed in Indonesian peatlands (3.7-87.8 mg CH<sub>4</sub>-C m<sup>-2</sup> d<sup>-1</sup>) (Couwenberg et al., 2010) and  
524 other Amazonian wetlands (7.1-390.0 mg CH<sub>4</sub>-C m<sup>-2</sup> d<sup>-1</sup>) (Bartlett et al., 1990; Bartlett et al.,  
525 1988; Devol et al., 1990; Devol et al., 1988). Although the ebullition data must be treated with  
526 caution because of the sampling methodology (see below), we observed an average ebullition  
527 flux of  $973.3 \pm 161.4$  mg CH<sub>4</sub>-C m<sup>-2</sup> d<sup>-1</sup>, spanning a range of 27 to 8,082 mg CH<sub>4</sub>-C m<sup>-2</sup> d<sup>-1</sup>.  
528 While data on ebullition from Amazonian wetlands are sparse, these values are broadly in-  
529 line with riverine and lake ecosystems sampled elsewhere (Bastviken et al., 2010; Smith et al.,  
530 2000; Sawakuchi et al., 2014). Ebullition-driven CH<sub>4</sub> uptake is not a commonly reported  
531 phenomena in other peatland studies because it is likely an artefact of chamber sampling  
532 methods; as a consequence, we do not discuss these data further here. To summarize, these  
533 data on diffusive CH<sub>4</sub> flux and ebullition suggest that peatlands in the Pastaza-Marañón  
534 foreland basin are strong contributors to the regional atmospheric budget of CH<sub>4</sub>, given that  
535 the four vegetation types sampled here represent the dominant cover types in the PMFB  
536 (Draper et al., 2014; Householder et al., 2012; Kelly et al., 2014; Lahteenoja and Page, 2011)

537

538 The overall trend in the diffusive flux data was towards greater temporal (i.e. seasonal)  
539 variability in diffusive CH<sub>4</sub> flux rather than strong spatial (i.e. inter-site) variability. For the  
540 pooled dataset, diffusive CH<sub>4</sub> emissions were significantly greater during the wet season than

541 the dry season, with emissions falling by approximately half from one season to the other (i.e.  
542  $51.1 \pm 7.0$  to  $27.3 \pm 2.7$  mg CH<sub>4</sub>-C m<sup>-2</sup> d<sup>-1</sup>). This is in contrast to the data on diffusive CH<sub>4</sub> flux  
543 among study sites, where statistical analyses indicate that there was a weak effect of  
544 vegetation type on CH<sub>4</sub> flux, that was only on the edge of statistical significance (i.e. ANCOVA;  
545  $P < 0.06$  for the vegetation effect term). For the ebullition data, while there was no significant  
546 difference among vegetation types nor between seasons, it is interesting to note that  
547 ebullition was more common for the two vegetation types – Mixed Palm Swamp and *M.*  
548 *flexuosa* palm swamp – that showed the highest rates of diffusive CH<sub>4</sub> flux (Figure 2, Table 2).  
549 In contrast, forested (short pole) and forested vegetation, which showed the lowest rates of  
550 diffusive CH<sub>4</sub> flux, also showed the lowest occurrence of ebullition (Figure 2, Table 2). This is  
551 broadly consistent with the notion that Mixed Palm Swamp and *M. flexuosa* palm swamp may  
552 produce more CH<sub>4</sub> than the other vegetation types.

553

554 On face value, these data on diffusive CH<sub>4</sub> flux suggest two findings; first, the relatively weak  
555 effect of vegetation type on diffusive CH<sub>4</sub> flux implies that patterns of CH<sub>4</sub> cycling are broadly  
556 similar among study sites. Second, the strong *overall* seasonal pattern suggests that – on the  
557 whole – these systems conform to our normative expectations of how peatlands function  
558 with respect to seasonal variations in hydrology and redox potential; i.e. enhanced CH<sub>4</sub>  
559 emissions during a more anoxic wet season (i.e. when water tables rise), and reduced CH<sub>4</sub>  
560 emissions during a more oxic dry season (i.e. when water tables fall). However, closer  
561 inspection of the data reveals that different vegetation types showed contrasting seasonal  
562 emission patterns (Table 3), challenging our basic assumptions about how these ecosystems  
563 function. For example, while forested (short pole) vegetation and *M. flexuosa* palm swamp

564 conformed to expected seasonal trends for methanogenic wetlands (i.e. higher wet season  
565 compared to dry season emissions), forested vegetation and mixed palm swamp showed the  
566 opposite pattern, with significantly greater CH<sub>4</sub> emissions during the dry season. The  
567 disaggregated data thus imply that the process-based controls on CH<sub>4</sub> fluxes may vary  
568 significantly among these different ecosystems, rather than being similar, leading to a  
569 divergence in seasonal flux patterns.

570

571 What may explain this pattern of seasonal divergence in CH<sub>4</sub> flux? One explanation is that CH<sub>4</sub>  
572 emissions from forested vegetation and mixed palm swamp, compared to the other two  
573 ecosystems, may be more strongly transport-limited during the wet season than the dry  
574 season. This interpretation is supported by the field data; forested vegetation and mixed palm  
575 swamp had the highest wet season water table levels, measuring  $110.8 \pm 9.3$  and  $183.7 \pm 1.7$   
576 cm, respectively (Table 2). In contrast, water table levels for forested (short pole) vegetation  
577 and *M. flexuosa* palm swamp in the wet season were 3-7 times lower, measuring only  $26.9 \pm$   
578  $0.5$  and  $37.2 \pm 1.7$  cm, respectively (Table 2). Moreover, a scatter plot of diffusive CH<sub>4</sub> flux  
579 against water table depth shows a peak in diffusive CH<sub>4</sub> emissions when water tables are  
580 between 30 to 40 cm above the surface, after which CH<sub>4</sub> emissions decline precipitously  
581 (Supplementary Online Materials Figure S2). Thus, the greater depth of overlying water in  
582 forested vegetation and mixed palm swamp may have exerted a much greater physical  
583 constraint on gas transport compared to the other two ecosystems. This interpretation is  
584 broadly consistent with studies from other ecosystems, which indicate that high or positive  
585 water tables may suppress CH<sub>4</sub> emissions from wetlands above a system-specific threshold  
586 (Couwenberg et al., 2010; Couwenberg et al., 2011).

587

588 However, transport limitation alone does not fully explain the difference in dry season CH<sub>4</sub>  
589 emissions among vegetation types. Forested vegetation and mixed palm swamp showed  
590 substantially higher dry season CH<sub>4</sub> emissions ( $47.2 \pm 5.4$  and  $85.5 \pm 26.4$  mg CH<sub>4</sub>-C m<sup>-2</sup> d<sup>-1</sup>,  
591 respectively) compared to forested (short pole) vegetation and *M. flexuosa* palm swamp ( $9.6$   
592  $\pm 2.6$  and  $25.5 \pm 2.9$  mg CH<sub>4</sub>-C m<sup>-2</sup> d<sup>-1</sup>, respectively), pointing to underlying differences in CH<sub>4</sub>  
593 production and oxidation among these ecosystems. One possibility is that dry season  
594 methanogenesis in forested vegetation and mixed palm swamp was greater than in the other  
595 two ecosystems, potentially driven by higher rates of C flow (Whiting and Chanton, 1993).  
596 This is plausible given that forested vegetation and mixed palm swamp tend to occur in more  
597 nutrient-rich parts of the Pastaza-Marañón foreland basin, whereas forested (short pole)  
598 vegetation and *M. flexuosa* palm swamp tend to dominate in more nutrient-poor areas  
599 (Lahteenoja et al., 2009a), leading to potential differences in rates of plant productivity and  
600 belowground C flow. Moreover, it is possible that the nutrient-rich vegetation may be able to  
601 utilize the higher concentration of nutrients, deposited during the flood pulse, during the  
602 Amazonian dry season (Morton et al., 2014; Saleska et al., 2016), with implications for overall  
603 ecosystem C throughput and CH<sub>4</sub> emissions. Of course, this interpretation does not preclude  
604 other explanations, such as differences in CH<sub>4</sub> transport rates among ecosystems (e.g. due to  
605 plant-facilitated transport or ebullition) (Panagala et al., 2013), or varying rates of CH<sub>4</sub>  
606 oxidation (Teh et al., 2005). However, these other possibilities cannot be explored further  
607 without recourse to more detailed process-level experiments. Forthcoming studies on the  
608 regulation of GHG fluxes at finer spatial scales (e.g. investigation of environmental gradients  
609 within individual study sites) or detailed diurnal studies of GHG exchange (Murphy *et al.*, in

610 prep.) will further deepen our understanding of the process controls on soil GHG flux from  
611 these peatlands, and shed light on these questions.

612

613 Finally, while the trends described here are intriguing, it is important to acknowledge some  
614 of the potential limitations of our data. First, given the uneven sampling pattern, it is possible  
615 that the values reported here do not fully represent the entire range of diffusive flux rates,  
616 especially for the more sparsely sampled habitats. However, given the large and statistically  
617 significant differences in CH<sub>4</sub> emissions between seasons, it is likely that the main trends that  
618 we have identified will hold true with more spatially-extensive sampling. Second, the data  
619 presented here represent a conservative underestimate of CH<sub>4</sub> emissions, because the low  
620 frequency, static chamber sampling approach that we utilized was unable to fully capture  
621 erratic ebullition events representatively (McClain et al., 2003). Although we attempted to  
622 quantify CH<sub>4</sub> ebullition within our static flux chambers, the sampling approach that we utilized  
623 was not the best-suited for representatively quantifying ebullition. Given the erratic or  
624 stochastic nature of ebullition, automated chamber measurements or an inverted “flux  
625 funnel” approach would have provided better estimates of ebullition (Strack et al., 2005).  
626 However, we lacked the resources to implement these approaches here. We also did not  
627 measure CH<sub>4</sub> emissions from the stems of woody plants, even though woody plants have been  
628 recently identified as an important point of atmospheric egress (Pangala et al., 2013). We did  
629 not have enough data on floristic composition or individual plant identities within our plots  
630 to develop a sampling design that would adequately represent plant-mediated fluxes from  
631 our study sites, nor the resources to implement a separate study of stem fluxes. Third and  
632 last, our data probably underestimate net CH<sub>4</sub> fluxes for the PMFB because we chose to

633 include fluxes with strong negative values (i.e. more than  $-10 \text{ mg CH}_4\text{-C m}^{-2} \text{ d}^{-1}$ ) in our  
634 calculation of mean diffusive flux rates. These observations are more negative than other  
635 values typically reported elsewhere in the tropical wetland literature (Bartlett et al.,  
636 1990; Bartlett et al., 1988; Devol et al., 1990; Devol et al., 1988; Couwenberg et al., 2010).  
637 However, they represent only a small proportion of our dataset (i.e. 7 %, or only 68 out of 980  
638 measurements), and inspection of our field notes and the data itself did not produce  
639 convincing reasons to exclude these observations (e.g. we found no evidence of irregularities  
640 during field sampling, and any chambers that showed statistically insignificant changes in  
641 concentration over time were removed during our quality control procedures). While  
642 headspace concentrations for these measurements were often elevated above mean  
643 tropospheric levels ( $>2 \text{ ppm}$ ), this in itself is not unusual in reducing environments that  
644 contain strong local sources of  $\text{CH}_4$  (Baldocchi et al., 2012). We did not see this as a reason to  
645 omit these values as local concentrations of  $\text{CH}_4$  are likely to vary naturally in methanogenic  
646 forest environments due to poor mixing in the understory and episodic ebullition events.  
647 Importantly, exclusion of these data did not alter the overall statistical trends reported above,  
648 and only produced slightly higher estimates of diffusive  $\text{CH}_4$  flux ( $41.6 \pm 3.2 \text{ mg CH}_4\text{-C m}^{-2} \text{ d}^{-1}$   
649 versus  $36.1 \pm 3.1 \text{ mg CH}_4\text{-C m}^{-2} \text{ d}^{-1}$ ).

650

## 651 **6.2 Western Amazonian peatlands as weak atmospheric sources of nitrous oxide**

652 The ecosystems sampled in this study were negligible atmospheric sources of  $\text{N}_2\text{O}$ , emitting  
653 only  $0.70 \pm 0.34 \mu\text{g N}_2\text{O-N m}^{-2} \text{ d}^{-1}$ , suggesting that peatlands in the Pastaza-Marañón foreland  
654 basin make little or no contribution to regional atmospheric budgets of  $\text{N}_2\text{O}$ . This is consistent  
655 with  $\text{N}_2\text{O}$  flux measurements from other forested tropical peatlands, where  $\text{N}_2\text{O}$  emissions

656 were also found to be relatively low (Inubushi et al., 2003; Couwenberg et al., 2010). No  
657 statistically significant differences in N<sub>2</sub>O flux were observed among study sites or between  
658 seasons, suggesting that these different peatlands may have similar patterns of N<sub>2</sub>O cycling.  
659 Interestingly, differences in N<sub>2</sub>O fluxes were not associated with the nutrient status of the  
660 peatland; i.e. more nutrient-rich ecosystems, such as forested vegetation and mixed palm  
661 swamp, did not show higher N<sub>2</sub>O fluxes than their nutrient-poor counterparts, such as  
662 forested (short pole) vegetation and *M. flexuosa* palm swamp. This may imply that N  
663 availability, one of the principal drivers of nitrification, denitrification, and N<sub>2</sub>O production  
664 (Groffman et al., 2009; Werner et al., 2007), may not be greater in nutrient-rich versus  
665 nutrient-poor ecosystems in this part of the Western Amazon. Alternatively, it is possible that  
666 even though N availability and N fluxes may differ between nutrient-rich and nutrient-poor  
667 systems, N<sub>2</sub>O yield may also vary such that net N<sub>2</sub>O emissions are not significantly different  
668 among study sites (Teh et al., 2014).

669

670 One potential source of concern are the negative N<sub>2</sub>O fluxes that we documented here. While  
671 some investigators have attributed negative fluxes to instrumental error (Cowan et al.,  
672 2014; Chapuis-Lardy et al., 2007), others have demonstrated that N<sub>2</sub>O consumption –  
673 particularly in wetland soils – is not an experimental artifact, but occurs due to the complex  
674 effects of redox, organic carbon content, nitrate availability, and soil transport processes on  
675 denitrification (Ye and Horwath, 2016; Yang et al., 2011; Wen et al., 2016; Schlesinger,  
676 2013; Teh et al., 2014; Chapuis-Lardy et al., 2007). Given the low redox potential and high  
677 carbon content of these soils, it is plausible that microbial N<sub>2</sub>O consumption is occurring,  
678 because these types of conditions have been found to be conducive for N<sub>2</sub>O uptake elsewhere  
679 (Ye and Horwath, 2016; Teh et al., 2014; Yang et al., 2011).

680

681

## 682 **7. CONCLUSIONS**

683 Our data suggest that peatlands in the Pastaza-Marañón foreland basin are strong sources of  
684 atmospheric CH<sub>4</sub> at a regional scale, and need to be better accounted for in CH<sub>4</sub> emissions  
685 inventories for the Amazon basin as a whole. In contrast, N<sub>2</sub>O fluxes were negligible,  
686 suggesting that these ecosystems are weak regional sources at best. Divergent or  
687 asynchronous seasonal emissions pattern for CH<sub>4</sub> among different vegetation types was  
688 intriguing, and challenges our underlying expectations of how tropical peatlands function.  
689 These data highlight the need for greater wet season sampling, particularly from ecosystems  
690 near river margins that may experience very high water tables (i.e. >40 cm). Moreover, these  
691 data also emphasize the need for more spatially-extensive sampling across both the Pastaza-  
692 Marañón foreland basin and the wider Amazon region as a whole, in order to establish if these  
693 asynchronous seasonal emission patterns are commonplace or specific to peatlands in the  
694 PMFB region. If CH<sub>4</sub> emission patterns for different peatlands in the Amazon are in fact  
695 asynchronous and decoupled from rainfall seasonality, then this may partially explain some  
696 of the heterogeneity in CH<sub>4</sub> source and sinks observed at the basin-wide scale (Wilson et al.,  
697 2016).

698

699

## 700 **8. AUTHOR CONTRIBUTION**



701 YAT secured the funding for this research, assisted in the planning and design of the  
702 experiment, and took the principal role in the analysis of the data and preparation of the  
703 manuscript. WAM planned and designed the experiment, collected the field data, analyzed  
704 the samples, and took a secondary role in data preparation, data analysis, and manuscript  
705 preparation. JCB, AB, and SEP supported the planning and design of the experiment, and  
706 provided substantive input into the writing of the manuscript. AB in particular took a lead role  
707 in developing the maps of our study sites in the PMFB.

708

709

## 710 **9. ACKNOWLEDGEMENTS**

711 The authors would like to acknowledge the UK Natural Environment Research Council for  
712 funding this research (NERC award number NE/I015469). We would like to thank MINAG and  
713 the Ministerio de Turismo in Iquitos for permits to conduct this research, the Instituto de  
714 Investigaciones de la Amazonía Peruana (IIAP) for logistical support, Peruvian rainforest  
715 villagers for their warm welcome and acceptance, Hugo Vasquez, Pierro Vasquez, Gian Carlo  
716 Padilla Tenazoa and Yully Rojas Reátegui for fieldwork assistance, Dr Outi Lahteenoja and Dr  
717 Ethan Householder for fieldwork planning, and Dr Paul Beaver of Amazonia Expeditions for  
718 lodging and logistical support. Our gratitude also goes to Alex Cumming for fieldwork support  
719 and laboratory assistance, Bill Hickin, Gemma Black, Adam Cox, Charlotte Langley, Kerry Allen,  
720 and Lisa Barber of the University of Leicester for all of their continued support. Thanks are  
721 also owed to Graham Hambley (St Andrews), Angus Calder (St Andrews), Viktoria Oliver  
722 (Aberdeen), Torsten Diem (Aberdeen), Tom Kelly (Leeds), and Freddie Draper Leeds) for their

723 help in the laboratory and with fieldwork planning. TD, VO, and two anonymous referees  
724 provided very helpful and constructive comments on earlier drafts of this manuscript. This  
725 publication is a contribution from the Scottish Alliance for Geoscience, Environment and  
726 Society (<http://www.sages.ac.uk>) and the UK Tropical Peatland Working Group  
727 (<https://tropicalpeat.wordpress.com>).

728

729

## 730 **10. REFERENCES**

731 Andriessse, J.: Nature and management of tropical peat soils, 59, Food & Agriculture Org.,  
732 1988.

733 Baggs, E. M.: A review of stable isotope techniques for N<sub>2</sub>O source partitioning in soils:  
734 Recent progress, remaining challenges and future considerations. , Rapid Communications  
735 in Mass Spectrometry 22, 1664-1672, 2008.

736 Baldocchi, D., Detto, M., Sonnentag, O., Verfaillie, J., Teh, Y. A., Silver, W., and Kelly, N. M.:  
737 The challenges of measuring methane fluxes and concentrations over a peatland pasture,  
738 Agric. For. Meteorol., 153, 177-187, <http://dx.doi.org/10.1016/j.agrformet.2011.04.013>, 2012.

739 Bartlett, K. B., Crill, P. M., Sebacher, D. I., Harriss, R. C., Wilson, J. O., and Melack, J. M.:  
740 METHANE FLUX FROM THE CENTRAL AMAZONIAN FLOODPLAIN, J. Geophys. Res.-Atmos.,  
741 93, 1571-1582, 1988.

742 Bartlett, K. B., Crill, P. M., Bonassi, J. A., Richey, J. E., and Harriss, R. C.: METHANE FLUX  
743 FROM THE AMAZON RIVER FLOODPLAIN - EMISSIONS DURING RISING WATER, J. Geophys.  
744 Res.-Atmos., 95, 16773-16788, 10.1029/JD095iD10p16773, 1990.

745 Bastviken, D., Santoro, A. L., Marotta, H., Pinho, L. Q., Calheiros, D. F., Crill, P., and Enrich-  
746 Prast, A.: Methane Emissions from Pantanal, South America, during the Low Water Season:  
747 Toward More Comprehensive Sampling, *Environ. Sci. Technol.*, 44, 5450-5455,  
748 10.1021/es1005048, 2010.

749 Belyea, L. R., and Baird, A. J.: Beyond "The limits to peat bog growth": Cross-scale feedback  
750 in peatland development, *Ecological Monographs*, 76, 299-322, 2006.

751 Blazewicz, S. J., Petersen, D. G., Waldrop, M. P., and Firestone, M. K.: Anaerobic oxidation of  
752 methane in tropical and boreal soils: Ecological significance in terrestrial methane cycling,  
753 *Journal of Geophysical Research: Biogeosciences*, 117, n/a-n/a, 10.1029/2011JG001864,  
754 2012.

755 Chapuis-Lardy, L., Wrage, N., Metay, A., Chotte, J.-L., and Bernoux, M.: Soils, a sink for N<sub>2</sub>O?  
756 A review, *Global Change Biology*, 13, 1-17, 10.1111/j.1365-2486.2006.01280.x, 2007.

757 Conrad, R.: Soil Microorganisms as Controllers of Atmospheric Trace Gases., *Microbiological*  
758 *Reviews*, 60, 609-640, 1996.

759 Couwenberg, J., Dommain, R., and Joosten, H.: Greenhouse gas fluxes from tropical  
760 peatlands in south-east Asia, *Global Change Biology*, 16, 1715-1732, 10.1111/j.1365-  
761 2486.2009.02016.x, 2010.

762 Couwenberg, J., Thiele, A., Tanneberger, F., Augustin, J., Bärish, S., Dubovik, D.,  
763 Liashchynskaya, N., Michaelis, D., Minke, M., Skuratovich, A., and Joosten, H.: Assessing  
764 greenhouse gas emissions from peatlands using vegetation as a proxy, *Hydrobiologia*, 674,  
765 67-89, 10.1007/s10750-011-0729-x, 2011.

766 Cowan, N. J., Famulari, D., Levy, P. E., Anderson, M., Reay, D. S., and Skiba, U. M.:  
767 Investigating uptake of N<sub>2</sub>O in agricultural soils using a high-precision dynamic  
768 chamber method, *Atmos. Meas. Tech.*, 7, 4455-4462, 10.5194/amt-7-4455-2014, 2014.

769 D'Amelio, M. T. S., Gatti, L. V., Miller, J. B., and Tans, P.: Regional N<sub>2</sub>O fluxes in Amazonia  
770 derived from aircraft vertical profiles, *Atmospheric Chemistry and Physics*, 9, 8785-8797,  
771 2009.

772 Devol, A. H., Richey, J. E., Clark, W. A., King, S. L., and Martinelli, L. A.: Methane emissions to  
773 the troposphere from the Amazon floodplain, *Journal of Geophysical Research:*  
774 *Atmospheres*, 93, 1583-1592, 10.1029/JD093iD02p01583, 1988.

775 Devol, A. H., Richey, J. E., Forsberg, B. R., and Martinelli, L. A.: SEASONAL DYNAMICS IN  
776 METHANE EMISSIONS FROM THE AMAZON RIVER FLOODPLAIN TO THE TROPOSPHERE, *J.*  
777 *Geophys. Res.-Atmos.*, 95, 16417-16426, 10.1029/JD095iD10p16417, 1990.

778 Draper, F. C., Roucoux, K. H., Lawson, I. T., Mitchard, E. T. A., Coronado, E. N. H., Lahteenoja,  
779 O., Montenegro, L. T., Sandoval, E. V., Zarate, R., and Baker, T. R.: The distribution and  
780 amount of carbon in the largest peatland complex in Amazonia, *Environmental Research*  
781 *Letters*, 9, 12, 10.1088/1748-9326/9/12/124017, 2014.

782 Firestone, M. K., Firestone, R. B., and Tiedge, J. M.: Nitrous oxide from soil denitrification:  
783 Factors controlling its biological production., *Science*, 208, 749-751, 1980.

784 Firestone, M. K., and Davidson, E. A.: Microbiological basis of NO and N<sub>2</sub>O production and  
785 consumption in soil, in: *Exchange of Trace Gases Between Terrestrial Ecosystems and the*  
786 *Atmosphere*, edited by: Andrae, M. O., and Schimel, D. S., John Wiley and Sons Ltd., New  
787 York, 7-21, 1989.

788 Groffman, P. M., Butterbach-Bahl, K., Fulweiler, R. W., Gold, A. J., Morse, J. L., Stander, E. K.,  
789 Tague, C., Tonitto, C., and Vidon, P.: Challenges to incorporating spatially and temporally  
790 explicit phenomena (hotspots and hot moments) in denitrification models, *Biogeochemistry*,  
791 93, 49-77, 10.1007/s10533-008-9277-5, 2009.

792 Hanson, R. S., and Hanson, T. E.: Methanotrophic Bacteria., *Microbiological Reviews*, 60,  
793 439-471, 1996.

794 Householder, J. E., Janovec, J., Tobler, M., Page, S., and Lähteenoja, O.: Peatlands of the  
795 Madre de Dios River of Peru: Distribution, Geomorphology, and Habitat Diversity, *Wetlands*,  
796 32, 359-368, 10.1007/s13157-012-0271-2, 2012.

797 Huang, J., Golombek, A., Prinn, R., Weiss, R., Fraser, P., Simmonds, P., Dlugokencky, E. J.,  
798 Hall, B., Elkins, J., Steele, P., Langenfelds, R., Krummel, P., Dutton, G., and Porter, L.:  
799 Estimation of regional emissions of nitrous oxide from 1997 to 2005 using multinetwork  
800 measurements, a chemical transport model, and an inverse method, *J. Geophys. Res.-*  
801 *Atmos.*, 113, 1-19, D17313  
802 10.1029/2007jd009381, 2008.

803 Jungkunst, H. F., and Fiedler, S.: Latitudinal differentiated water table control of carbon  
804 dioxide, methane and nitrous oxide fluxes from hydromorphic soils: feedbacks to climate  
805 change, *Global Change Biology*, 13, 2668-2683, 10.1111/j.1365-2486.2007.01459.x, 2007.

806 Keller, M., Kaplan, W. A., and Wofsy, S. C.: EMISSIONS OF N<sub>2</sub>O, CH<sub>4</sub> AND CO<sub>2</sub> FROM  
807 TROPICAL FOREST SOILS, *J. Geophys. Res.-Atmos.*, 91, 1791-1802,  
808 10.1029/JD091iD11p11791, 1986.

809 Kelly, T. J., Baird, A. J., Roucoux, K. H., Baker, T. R., Honorio Coronado, E. N., Ríos, M., and  
810 Lawson, I. T.: The high hydraulic conductivity of three wooded tropical peat swamps in  
811 northeast Peru: measurements and implications for hydrological function, *Hydrological*  
812 *Processes*, 28, 3373-3387, 10.1002/hyp.9884, 2014.

813 Kirschke, S., Bousquet, P., Ciais, P., Saunois, M., Canadell, J. G., Dlugokencky, E. J.,  
814 Bergamaschi, P., Bergmann, D., Blake, D. R., Bruhwiler, L., Cameron-Smith, P., Castaldi, S.,

815 Chevallier, F., Feng, L., Fraser, A., Heimann, M., Hodson, E. L., Houweling, S., Josse, B.,  
816 Fraser, P. J., Krummel, P. B., Lamarque, J. F., Langenfelds, R. L., Le Quere, C., Naik, V.,  
817 O'Doherty, S., Palmer, P. I., Pison, I., Plummer, D., Poulter, B., Prinn, R. G., Rigby, M.,  
818 Ringeval, B., Santini, M., Schmidt, M., Shindell, D. T., Simpson, I. J., Spahni, R., Steele, L. P.,  
819 Strode, S. A., Sudo, K., Szopa, S., van der Werf, G. R., Voulgarakis, A., van Weele, M., Weiss,  
820 R. F., Williams, J. E., and Zeng, G.: Three decades of global methane sources and sinks,  
821 *Nature Geoscience*, 6, 813-823, 10.1038/ngeo1955, 2013.

822 Lahteenoja, O., Ruokolainen, K., Schulman, L., and Alvarez, J.: Amazonian floodplains  
823 harbour minerotrophic and ombrotrophic peatlands, *Catena*, 79, 140-145,  
824 10.1016/j.catena.2009.06.006, 2009a.

825 Lahteenoja, O., Ruokolainen, K., Schulman, L., and Oinonen, M.: Amazonian peatlands: an  
826 ignored C sink and potential source, *Global Change Biology*, 15, 2311-2320, 10.1111/j.1365-  
827 2486.2009.01920.x, 2009b.

828 Lahteenoja, O., and Page, S.: High diversity of tropical peatland ecosystem types in the  
829 Pastaza-Maranon basin, Peruvian Amazonia, *Journal of Geophysical Research-*  
830 *Biogeosciences*, 116, 14, 10.1029/2010jg001508, 2011.

831 Lahteenoja, O., Reategui, Y. R., Rasanen, M., Torres, D. D., Oinonen, M., and Page, S.: The  
832 large Amazonian peatland carbon sink in the subsiding Pastaza-Maranon foreland basin,  
833 Peru, *Global Change Biology*, 18, 164-178, 10.1111/j.1365-2486.2011.02504.x, 2012.

834 Lavelle, P., Rodriguez, N., Arguello, O., Bernal, J., Botero, C., Chaparro, P., Gomez, Y.,  
835 Gutierrez, A., Hurtado, M. D., Loaiza, S., Pullido, S. X., Rodriguez, E., Sanabria, C., Velasquez,  
836 E., and Fonte, S. J.: Soil ecosystem services and land use in the rapidly changing Orinoco  
837 River Basin of Colombia, *Agriculture Ecosystems & Environment*, 185, 106-117,  
838 10.1016/j.agee.2013.12.020, 2014.

839 Liengaard, L., Nielsen, L. P., Revsbech, N. P., Priem, A., Elberling, B., Enrich-Prast, A., and  
840 Kuhl, M.: Extreme emission of N<sub>2</sub>O from tropical wetland soil (Pantanal, South America),  
841 *Frontiers in Microbiology*, 3, 13, 10.3389/fmicb.2012.00433, 2013.

842 Limpens, J., Berendse, F., Blodau, C., Canadell, J. G., Freeman, C., Holden, J., Roulet, N.,  
843 Rydin, H., and Schaepman-Strub, G.: Peatlands and the carbon cycle: from local processes to  
844 global implications – a synthesis, *Biogeosciences*, 5, 1475–1491, 2008.

845 Marani, L., and Alvalá, P. C.: Methane emissions from lakes and floodplains in Pantanal,  
846 Brazil, *Atmospheric Environment*, 41, 1627-1633,  
847 <http://dx.doi.org/10.1016/j.atmosenv.2006.10.046>, 2007.

848 McClain, M. E., Boyer, E. W., Dent, C. L., Gergel, S. E., Grimm, N. B., Groffman, P. M., Hart, S.  
849 C., Harvey, J. W., Johnston, C. A., Mayorga, E., McDowell, W. H., and Pinay, G.:  
850 Biogeochemical hot spots and hot moments at the interface of terrestrial and aquatic  
851 ecosystems, *Ecosystems*, 6, 301-312, 10.1007/s10021-003-0161-9, 2003.

852 Melack, J. M., Hess, L. L., Gastil, M., Forsberg, B. R., Hamilton, S. K., Lima, I. B. T., and Novo,  
853 E.: Regionalization of methane emissions in the Amazon Basin with microwave remote  
854 sensing, *Global Change Biology*, 10, 530-544, 10.1111/j.1529-8817.2003.00763.x, 2004.

855 Melton, J. R., Wania, R., Hodson, E. L., Poulter, B., Ringeval, B., Spahni, R., Bohn, T., Avis, C.  
856 A., Beerling, D. J., Chen, G., Eliseev, A. V., Denisov, S. N., Hopcroft, P. O., Lettenmaier, D. P.,  
857 Riley, W. J., Singarayer, J. S., Subin, Z. M., Tian, H., Zurcher, S., Brovkin, V., van Bodegom, P.  
858 M., Kleinen, T., Yu, Z. C., and Kaplan, J. O.: Present state of global wetland extent and  
859 wetland methane modelling: conclusions from a model inter-comparison project  
860 (WETCHIMP), *Biogeosciences*, 10, 753-788, 10.5194/bg-10-753-2013, 2013.

861 Morley, N., and Baggs, E. M.: Carbon and oxygen controls on N<sub>2</sub>O and N<sub>2</sub> production during  
862 nitrate reduction, *Soil Biol. Biochem.*, 42, 1864-1871, 10.1016/j.soilbio.2010.07.008, 2010.

863 Morton, D. C., Nagol, J., Carabajal, C. C., Rosette, J., Palace, M., Cook, B. D., Vermote, E. F.,  
864 Harding, D. J., and North, P. R. J.: Amazon forests maintain consistent canopy structure and  
865 greenness during the dry season, *Nature*, 506, 221-224, 10.1038/nature13006  
866 <http://www.nature.com/nature/journal/v506/n7487/abs/nature13006.html> - supplementary-  
867 [information](#), 2014.

868 Nisbet, E. G., Dlugokencky, E. J., and Bousquet, P.: Methane on the Rise—Again, *Science*,  
869 343, 493-495, 10.1126/science.1247828, 2014.

870 Pangala, S. R., Moore, S., Hornibrook, E. R. C., and Gauci, V.: Trees are major conduits for  
871 methane egress from tropical forested wetlands, *New Phytologist*, 197, 524-531,  
872 10.1111/nph.12031, 2013.

873 Pett-Ridge, J., Petersen, D. G., Nuccio, E., and Firestone, M. K.: Influence of oxic/anoxic  
874 fluctuations on ammonia oxidizers and nitrification potential in a wet tropical soil, *FEMS*  
875 *Microbiol. Ecol.*, 85, 179-194, 10.1111/1574-6941.12111, 2013.

876 Prosser, J. I., and Nicol, G. W.: Relative contributions of archaea and bacteria to aerobic  
877 ammonia oxidation in the environment, *Environ. Microbiol.*, 10, 2931-2941, 10.1111/j.1462-  
878 2920.2008.01775.x, 2008.

879 Saikawa, E., Schlosser, C. A., and Prinn, R. G.: Global modeling of soil nitrous oxide emissions  
880 from natural processes, *Global Biogeochemical Cycles*, 27, 972-989, 10.1002/gbc.20087,  
881 2013.

882 Saikawa, E., Prinn, R. G., Dlugokencky, E., Ishijima, K., Dutton, G. S., Hall, B. D., Langenfelds,  
883 R., Tohjima, Y., Machida, T., Manizza, M., Rigby, M., O'Doherty, S., Patra, P. K., Harth, C. M.,  
884 Weiss, R. F., Krummel, P. B., van der Schoot, M., Fraser, P. J., Steele, L. P., Aoki, S.,  
885 Nakazawa, T., and Elkins, J. W.: Global and regional emissions estimates for N<sub>2</sub>O,  
886 *Atmospheric Chemistry and Physics*, 14, 4617-4641, 10.5194/acp-14-4617-2014, 2014.



887 Saleska, S. R., Wu, J., Guan, K., Araujo, A. C., Huete, A., Nobre, A. D., and Restrepo-Coupe,  
888 N.: Dry-season greening of Amazon forests, *Nature*, 531, E4-E5, 10.1038/nature16457, 2016.

889 Sawakuchi, H. O., Bastviken, D., Sawakuchi, A. O., Krusche, A. V., Ballester, M. V. R., and  
890 Richey, J. E.: Methane emissions from Amazonian Rivers and their contribution to the global  
891 methane budget, *Global Change Biology*, 20, 2829-2840, 10.1111/gcb.12646, 2014.

892 Schlesinger, W. H.: An estimate of the global sink for nitrous oxide in soils, *Global Change*  
893 *Biology*, 19, 2929-2931, 10.1111/gcb.12239, 2013.

894 Schulman, L., Ruokolainen, K., and Tuomisto, H.: Parameters for global ecosystem models,  
895 *Nature*, 399, 535-536, 1999.

896 Silver, W., Lugo, A., and Keller, M.: Soil oxygen availability and biogeochemistry along  
897 rainfall and topographic gradients in upland wet tropical forest soils., *Biogeochemistry*, 44,  
898 301-328, 1999.

899 Silver, W. L., Herman, D. J., and Firestone, M. K. S.: Dissimilatory Nitrate Reduction to  
900 Ammonium in Upland Tropical Forest Soils., *Ecology*, 82, 2410-2416, 2001.

901 Sjögersten, S., Black, C. R., Evers, S., Hoyos-Santillan, J., Wright, E. L., and Turner, B. L.:  
902 Tropical wetlands: A missing link in the global carbon cycle?, *Global Biogeochemical Cycles*,  
903 28, 1371-1386, 10.1002/2014GB004844, 2014.

904 Smith, L. K., Lewis, W. M., Chanton, J. P., Cronin, G., and Hamilton, S. K.: Methane emissions  
905 from the Orinoco River floodplain, Venezuela., *Biogeochemistry*, 51, 113-140, 2000.

906 Strack, M., Kellner, E., and Waddington, J. M.: Dynamics of biogenic gas bubbles in peat and  
907 their effects on peatland biogeochemistry, *Global Biogeochemical Cycles*, 19, n/a-n/a,  
908 10.1029/2004GB002330, 2005.

909 Teh, Y. A., Silver, W. L., and Conrad, M. E.: Oxygen effects on methane production and  
910 oxidation in humid tropical forest soils, *Global Change Biology*, 11, 1283-1297,  
911 10.1111/j.1365-2486.2005.00983.x, 2005.

912 Teh, Y. A., and Silver, W. L.: Effects of soil structure destruction on methane production and  
913 carbon partitioning between methanogenic pathways in tropical rain forest soils, *Journal of*  
914 *Geophysical Research: Biogeosciences*, 111, n/a-n/a, 10.1029/2005JG000020, 2006.

915 Teh, Y. A., Silver, W. L., Conrad, M. E., Borglin, S. E., and Carlson, C. M.: Carbon isotope  
916 fractionation by methane-oxidizing bacteria in tropical rain forest soils, *Journal of*  
917 *Geophysical Research-Biogeosciences*, 111, 10.1029/2005jg000053, 2006.

918 Teh, Y. A., Dubinsky, E. A., Silver, W. L., and Carlson, C. M.: Suppression of methanogenesis  
919 by dissimilatory Fe(III)-reducing bacteria in tropical rain forest soils: implications for  
920 ecosystem methane flux, *Global Change Biology*, 14, 413-422, 10.1111/j.1365-  
921 2486.2007.01487.x, 2008.

922 Teh, Y. A., Silver, W. L., Sonnentag, O., Detto, M., Kelly, M., and Baldocchi, D. D.: Large  
923 Greenhouse Gas Emissions from a Temperate Peatland Pasture, *Ecosystems*, 14, 311-325,  
924 10.1007/s10021-011-9411-4, 2011.

925 Teh, Y. A., Diem, T., Jones, S., Huaraca Quispe, L. P., Baggs, E., Morley, N., Richards, M.,  
926 Smith, P., and Meir, P.: Methane and nitrous oxide fluxes across an elevation gradient in the  
927 tropical Peruvian Andes, *Biogeosciences*, 11, 2325-2339, 10.5194/bg-11-2325-2014, 2014.

928 von Fischer, J., and Hedin, L.: Separating methane production and consumption with a field-  
929 based isotope dilution technique., *Global Biogeochemical Cycles*, 16, 1-13,  
930 10.1029/2001GB001448, 2002.

931 von Fischer, J. C., and Hedin, L. O.: Controls on soil methane fluxes: Tests of biophysical  
932 mechanisms using stable isotope tracers, *Global Biogeochemical Cycles*, 21, 9, Gb2007

933 10.1029/2006gb002687, 2007.

934 Wen, Y., Chen, Z., Dannenmann, M., Carminati, A., Willibald, G., Kiese, R., Wolf, B.,  
935 Veldkamp, E., Butterbach-Bahl, K., and Corre, M. D.: Disentangling gross N<sub>2</sub>O production  
936 and consumption in soil, *Sci Rep*, 6, 8, 10.1038/srep36517, 2016.

937 Werner, C., Butterbach-Bahl, K., Haas, E., Hickler, T., and Kiese, R.: A global inventory of N<sub>2</sub>O  
938 emissions from tropical rainforest soils using a detailed biogeochemical model, *Global*  
939 *Biogeochemical Cycles*, 21, 1-18, Gb3010

940 10.1029/2006gb002909, 2007.

941 Whalen, S. C.: Biogeochemistry of methane exchange between natural wetlands and the  
942 atmosphere, *Environ. Eng. Sci.*, 22, 73-94, 10.1089/ees.2005.22.73, 2005.

943 Whiting, G. J., and Chanton, J. P.: Primary production control of methane emission from  
944 wetlands., *Nature*, 364, 794-795, 1993.

945 Wilson, C., Gloor, M., Gatti, L. V., Miller, J. B., Monks, S. A., McNorton, J., Bloom, A. A.,  
946 Basso, L. S., and Chipperfield, M. P.: Contribution of regional sources to atmospheric  
947 methane over the Amazon Basin in 2010 and 2011, *Global Biogeochem. Cycles*, 30, 400–420,  
948 10.1002/2015GB005300, 2016.

949 Wright, E. L., Black, C. R., Cheesman, A. W., Drage, T., Large, D., Turner, B. L., and  
950 Sjögersten, S.: Contribution of subsurface peat to CO<sub>2</sub> and CH<sub>4</sub> fluxes in a neotropical  
951 peatland, *Global Change Biology*, 17, 2867-2881, 10.1111/j.1365-2486.2011.02448.x, 2011.

952 Yang, W. H., Teh, Y. A., and Silver, W. L.: A test of a field-based N-15-nitrous oxide pool  
953 dilution technique to measure gross N<sub>2</sub>O production in soil, *Global Change Biology*, 17,  
954 3577-3588, 10.1111/j.1365-2486.2011.02481.x, 2011.

955 Ye, R., and Horwath, W. R.: Nitrous oxide uptake in rewetted wetlands with contrasting soil  
956 organic carbon contents, *Soil Biology and Biochemistry*, 100, 110-117,  
957 <http://dx.doi.org/10.1016/j.soilbio.2016.06.009>, 2016.

958

959 **11. TABLES AND FIGURES**

960 **Table 1.** Site characteristics including field site location, nutrient status, plot and flux chamber  
 961 replication

Vegetation type	Site name	Nutrient status*	Latitude (S)	Longitude (W)	Plots	Flux chambers
Forested	Buena Vista	Rich	4°14'45.60"S	73°12'0.20"W	21	105
Forested (short pole)	San Jorge (centre)	Poor	4°03'35.95"S	73°12'01.13"W	6	28
Forested (short pole)	Miraflores	Poor	4°28'16.59"S	74° 4'39.95"W	41	204
M. flexuosa Palm Swamp	Quistococha	Intermediate	3°49'57.61"S	73°12'01.13"W	135	668
M. flexuosa Palm Swamp	San Jorge (edge)	Intermediate	4°03'18.83"S	73°10'16.80"W	18	86
Mixed palm swamp	Charo	Rich	4°16'21.80"S	73°15'27.80"W	18	90

962 \*After Householder et al. 2012, Lahteenoja et al. 2009a, and Lahteenoja et al. 2009b

963

964 **Table 2.** Proportion of observations for each vegetation type that showed evidence of  
 965 ebullition, mean rates of ebullition and ebullition-driven CH<sub>4</sub> uptake. Values represent  
 966 means and standard errors.

Vegetation Type	Percentage of observations (%)	Ebullition (mg CH <sub>4</sub> -C m <sup>-2</sup> d <sup>-1</sup> )		Ebullition-driven uptake (mg CH <sub>4</sub> -C m <sup>-2</sup> d <sup>-1</sup> )	
		Wet Season	Dry Season	Wet Season	Dry Season
Forested	10.5	0	0	0	-136.4 ± 0.1
Forested (short pole)	6.9	994.6 ± 293.2	512.5 ± 153.0	-95.8 ± 0.0	-245.5 ± 48.9
<i>M. flexuosa</i> Palm Swamp	16.7	1192.0 ± 305.7	994.3 ± 237.3	-869.4 ± 264.8	-401.4 ± 59.9
Mixed Palm Swamp	12.2	0	733.6 ± 313.1	0	-464.4 ± 565.9

967

968 **Table 3.** Environmental variables for each vegetation type for the wet and dry season.  
 969 Values reported here are means and standard errors. Lower case letters indicate significant  
 970 differences among vegetation types within the wet or dry season (Fisher's LSD,  $P < 0.05$ ).

Vegetation Type	Peat Temperature (°C)		Air Temperature (°C)		Conductivity ( $\mu\text{S m}^{-2}$ )		Dissolved Oxygen (%)		Water Table Level (cm)		pH	
	Wet Season	Dry Season	Wet Season	Dry Season	Wet Season	Dry Season	Wet Season	Dry Season	Wet Season	Dry Season	Wet Season	Dry Season
Forested	26.1 ± 0.1a	24.7 ± 0.0a	28.8 ± 0.7a	26.4 ± 0.3a	79.0 ± 5.9a	75.9 ± 5.7a	0.2 ± 0.1a	18.9 ± 4.4a	110.8 ± 9.3a	-13.2 ± 0.7a	5.88 ± 0.15a	6.31 ± 0.04a
Forested (short pole)	25.2 ± 0.0b	24.8 ± 0.1a	27.6 ± 0.1b	27.5 ± 0.1b	21.0 ± 0.0b	48.5 ± 4.8b	4.4 ± 0.0a	33.1 ± 2.6b	26.9 ± 0.5b	-4.7 ± 0.4b	4.88 ± 0.01b	3.8 ± 0.03b
M. flexuosa	25.6 ± 0.0b	25.3 ± 0.1a	26.3 ± 0.1b	26.4 ± 0.1b	45.9 ± 0.0b	51.9 ± 19.4 ±	19.4 ± 17.3 ±	17.3 ± 37.2 ±	6.1 ± 5.04 ±	6.1 ± 5.04 ±	5.04 ± 5.49 ±	5.49 ±
Palm Swamp	0.6c	0.1b	0.1c	0.1a	2.1c	1.8b	1.3b	1.5a	1.7c	1.3c	0.03c	0.03c
Mixed Palm	26.0 ±	25.0 ±	26.1 ±	28.2 ±	100.0 ±	206.4 ±	0.0 ±	0.0 ±	183.7 ±	-2.4 ±	6.1 ±	6.82 ±
Swamp	0.0a	0.1ab	0.1c	0.3b	0.2d	4.2c	0.0a	0.0c	1.7d	0.3b	0.03a	0.02d

971

972 **Table 4.** Trace gas fluxes for each vegetation type for the wet and dry season. Values reported  
 973 here are means and standard errors. Upper case letters indicate significant differences in gas  
 974 flux between seasons with a vegetation type, while lower case letters indicate significant  
 975 differences among vegetation types within a season (Fisher's LSD,  $P < 0.05$ ).

Vegetation Type	Methane Flux (mg CH <sub>4</sub> -C m <sup>-2</sup> d <sup>-1</sup> )		Nitrous Oxide Flux (µg N <sub>2</sub> O-N m <sup>-2</sup> d <sup>-1</sup> )	
	Wet Season	Dry Season	Wet Season	Dry Season
Forested	6.7 ± 1.0Aa	47.2 ± 5.4Ba	2.54 ± 1.48	-1.16 ± 1.20
Forested (short pole)	60.4 ± 9.1Ab	18.8 ± 2.6Bb	1.16 ± 0.54	-0.42 ± 0.90
<i>M. flexuosa</i> Palm Swamp	46.7 ± 8.4Ac	28.3 ± 2.6Bc	1.14 ± 0.35	0.92 ± 0.61
Mixed Palm Swamp	6.1 ± 1.3Aa	64.2 ± 12.1Ba	1.45 ± 0.79	-0.80 ± 0.79

976



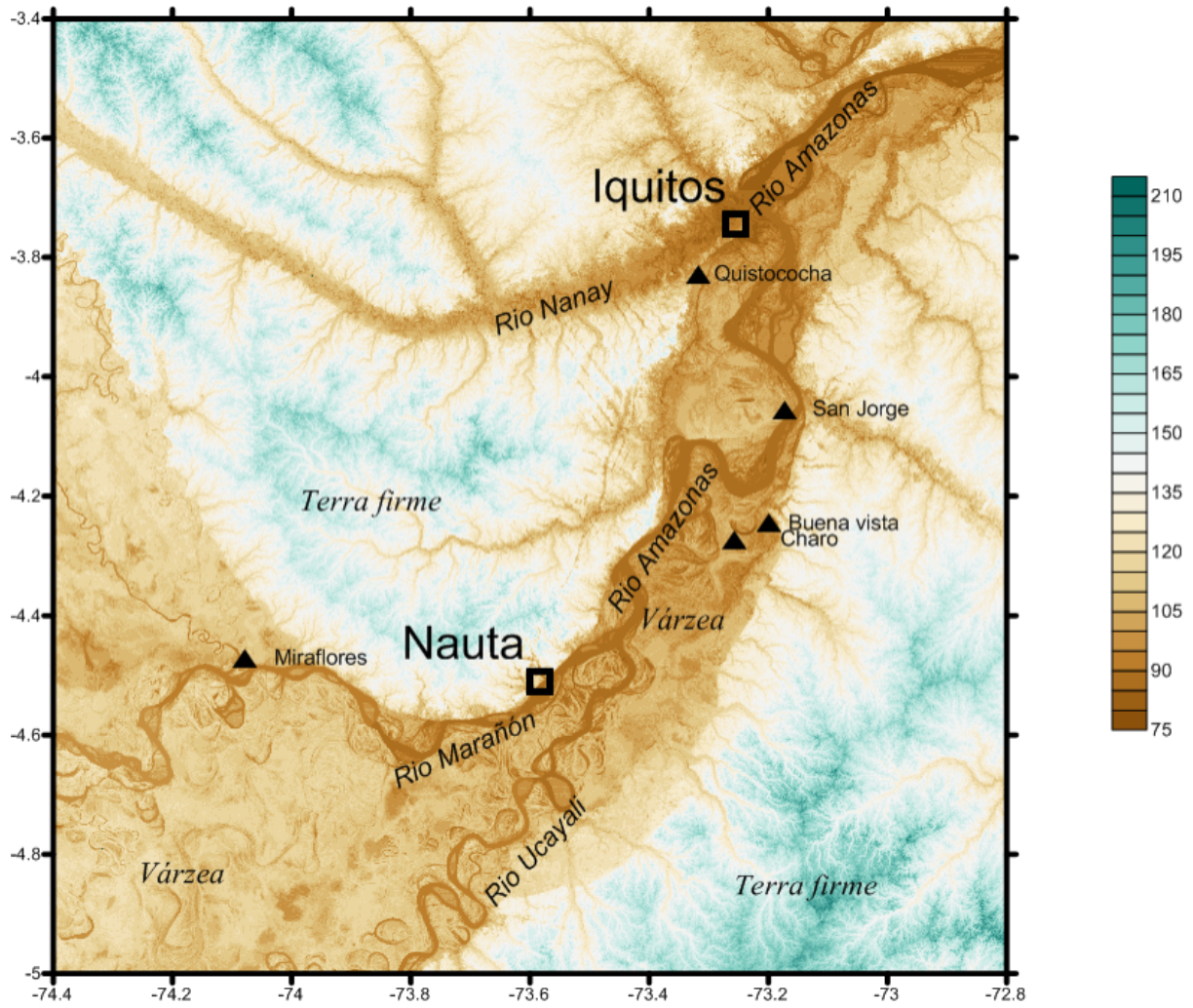
977 **Figure Captions**

978 **Figure 1.** Map of the study region and field sites. The colour scale to the right of the map  
979 denotes elevation in meters above sea level (m a.s.l.). Tan and brown tones indicate peatland  
980 areas.

981

982 **Figure 2.** Net diffusive **(a)** methane ( $\text{CH}_4$ ) and **(b)** nitrous oxide ( $\text{N}_2\text{O}$ ) fluxes by vegetation type.  
983 Error bars denote standard errors.

984 **Figure 1**



985

